

# Control of the Stability, Electron-Transfer Kinetics, and pH-Dependent Energetics of Si/H<sub>2</sub>O Interfaces through Methyl Termination of Si(111) Surfaces

Thomas W. Hamann and Nathan S. Lewis\*

Division of Chemistry and Chemical Engineering, Beckman Institute and Kavli Nanoscience Institute, 210 Noyes Laboratory, 127-72, California Institute of Technology, Pasadena, California 91125

Received: July 12, 2006; In Final Form: September 22, 2006

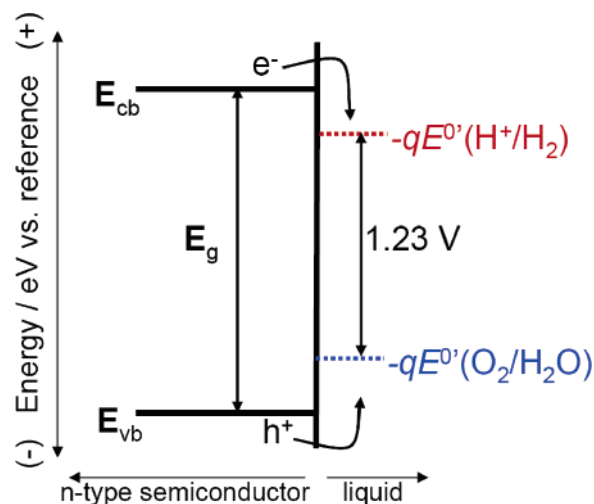
Methyl-terminated, n-type, (111)-oriented Si surfaces were prepared via a two-step chlorination-alkylation method. This surface modification passivated the Si surface toward electrochemical oxidation and thereby allowed measurements of interfacial electron-transfer processes in contact with aqueous solutions. The resulting semiconductor/liquid junctions exhibited interfacial kinetics behavior in accord with the ideal model of a semiconductor/liquid junction. In contrast to the behavior of H-terminated Si(111) surfaces, current density vs. potential measurements of CH<sub>3</sub>-terminated Si(111) surfaces in contact with an electron acceptor having a pH-independent redox potential (methyl viologen<sup>2+/+</sup>) were used to verify that the band edges of the modified Si electrode were fixed with respect to changes in solution pH. The results provide strong evidence that the energetics of chemically modified Si interfaces can be fixed with respect to pH and show that the band-edge energies of Si can be tuned independently of pH-derived variations in the electrochemical potential of the solution redox species.

## I. Introduction

The positions of the band edges of photoelectrodes must be controlled to enable water splitting and other desirable photoelectrochemical reactions at semiconductor/liquid interfaces.<sup>1,2</sup> For water splitting, for example, the energies of the bottom of the conduction band and the top of the valence band, respectively, need to be positioned appropriately with respect to the electrochemical potentials of the H<sup>+</sup>/H<sub>2</sub> and O<sub>2</sub>/H<sub>2</sub>O redox couples (Scheme 1).<sup>1</sup> The electrochemical potentials of the H<sup>+</sup>/H<sub>2</sub> and O<sub>2</sub>/H<sub>2</sub>O systems can, of course, be manipulated by changing the pH of the solution.<sup>3</sup> It is well-documented, however, that such pH variation does not in general affect the energetics of the semiconductor/liquid interface, because the band-edge positions of the semiconductor surface are also sensitive to pH.<sup>4–6</sup> The need to manipulate the band-edge positions has prompted “band-edge engineering” approaches in which materials with different band gaps are layered onto desired photoactive materials, in attempts to shift the energetics of the semiconductor into the appropriate positions.<sup>7</sup> We describe herein another approach to control the interfacial energetics of photoelectrodes, in which covalent chemical modification of the surface is used to eliminate the pH dependence of the band edges, allowing pH control of the electrolyte to manipulate the energetics of the bands of the solid relative to the electrochemical potential of the solution.

Metal oxide photoelectrodes are well-known to display a Nernstian dependence of their flat-band potential,  $E_{fb}$ , on pH.<sup>4–6,8</sup> The 1.1 eV band-gap of Si is better matched to the solar spectrum than that of most metal oxides,<sup>2</sup> and Si could be

SCHEME 1. Energy vs Distance for an Idealized n-Type Semiconductor for Water Splitting in Contact with an Aqueous Solution<sup>a</sup>



<sup>a</sup> The conduction-band and valence-band edges,  $E_{cb}$  and  $E_{vb}$ , respectively, separated by a band gap energy,  $E_g$ , must straddle the formal potentials  $E^{\circ}(\text{H}^+/\text{H}_2)$  and  $E^{\circ}(\text{O}_2/\text{H}_2\text{O})$  for the reduction (red) and oxidation (blue), respectively, of water.

used in a dual-junction or heterojunction type system for water splitting if its band-edge positions could be appropriately controlled. Si, however, readily oxidizes in the presence of mildly oxidizing redox species in water,<sup>9</sup> introducing both electrochemical instability and an oxide layer whose protonation/deprotonation equilibria impart pH sensitivity to the band-edge positions of Si/H<sub>2</sub>O interfaces. For example, shifts of  $E_{fb}$  of  $-33$

\* Corresponding author. E-mail: nslewis@caltech.edu

mV/pH unit,<sup>10</sup>  $-59$  mV/pH unit,<sup>11</sup> as well as nonlinear shifts of  $E_{fb}$  with variations in pH,<sup>9</sup> have been reported for Si/H<sub>2</sub>O interfaces.

In this work, we describe the covalent modification of Si surfaces via a two-step chlorination–methylation method<sup>12</sup> to introduce kinetically stable CH<sub>3</sub>–Si bonds onto Si surfaces. This process eliminates the pH dependence of the Si band-edge positions, and additionally facilitates use of the Si under conditions in which it otherwise would be rapidly oxidized to produce pH-dependent surface potentials. This methylation process additionally allows for the experimental measurement of the interfacial electron-transfer kinetics in media which can not be probed at reactive, oxidizable, H-terminated Si surfaces, and has produced a system which reveals “ideal” kinetics behavior at the semiconductor/liquid contact. The ability to control the band-edge positions, and to introduce, or eliminate, a pH-dependence of Si surfaces through molecular level control, without introducing deleterious levels of surface states, is of obvious relevance to Si chem-FETs (field-effect transistors),<sup>13</sup> light-addressable potentiometric sensor devices,<sup>14</sup> Si nanowire sensors used in chemical and biological applications,<sup>15</sup> and has implications in a variety of other applications of semiconductor/liquid interfaces.

## II. Experimental Section

The (111)-oriented, n-type, Si single crystals (Crysteco Inc.) had a resistivity of  $3.7 \Omega \text{ cm}$ , as determined from four-point probe measurements. The samples were H-terminated by etching for 20 min in an 11 M (40% by weight) NH<sub>4</sub>F(aq) solution that was purged with Ar.<sup>12,16,17</sup> CH<sub>3</sub>-terminated Si samples were prepared by chlorinating H–Si(111) samples with PCl<sub>5</sub> in chlorobenzene at 100 °C for 1 h, followed by heating at 70 °C for 14 – 18 h in a 1 M CH<sub>3</sub>MgBr solution, as described previously.<sup>12,16</sup> Ga–In eutectic was used as an ohmic contact and silver print was used to connect the Ga–In to a tinned copper wire. Paraffin wax was used to seal the electrode assembly in a glass tube. The resulting electrode areas, typically 0.2–0.5 cm<sup>2</sup>, were determined by digitizing photographs of a microruler and of the exposed Si surface.

Methyl viologen (MV<sup>2+</sup>) dichloride was purchased from Aldrich and was used as received. Potassium chloride (pH = 1.4), phthalate (pH = 3.8), phosphate (pH = 6.8), borax (pH = 9.0), and phosphate (pH = 11.0) buffers were prepared by literature methods.<sup>18</sup> The ionic strength of all solutions was adjusted to 1.0 M by the addition of KCl. The pH was measured using a VWR Scientific model 8010 pH meter.

Electrochemical measurements were performed with a Schlumberger Instruments model SI1287 potentiostat. All potentials were referenced to a standard calomel electrode (SCE). All solutions were purged with Ar before each measurement, and measurements were performed under an Ar atmosphere in the dark. X-ray photoelectron spectroscopic (XPS) data were obtained using a 1487 eV Al K $\alpha$  source, as described previously.<sup>16</sup>

## III. Results and Discussion

Figure 1 depicts the current density,  $J$ , vs. applied potential,  $E$ , data for CH<sub>3</sub>–Si(111) and H–Si(111) electrodes, respectively, in the dark in contact with 10 mM MV<sup>2+</sup>(aq). Si has a high overpotential for H<sub>2</sub> evolution, so H<sub>2</sub> production does not interfere with observation of the reduction of MV<sup>2+</sup> in the potential range of interest (Figure 1).<sup>19–22</sup> The initial scan of the H-terminated electrode displayed in Figure 1 was very similar to that of the CH<sub>3</sub>-terminated electrode, but the current density of the H–Si(111) surface decayed quite rapidly there-

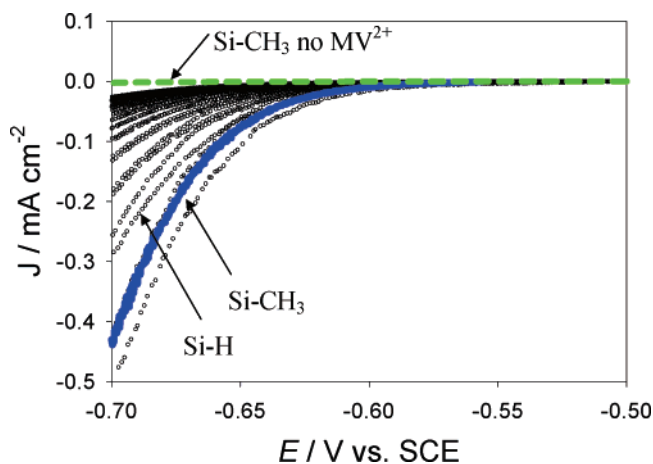


**Figure 1.** Plots of 20 scans of the current density ( $J$ ) vs applied potential ( $E$ ) at  $10 \text{ mV s}^{-1}$  for H-terminated Si(111) (black open circles) and CH<sub>3</sub>-terminated Si(111) (solid line) electrodes in the dark in contact with a 10 mM MV<sup>2+</sup> buffered at pH 11.0. Also shown is a  $J$ – $E$  curve for CH<sub>3</sub>-terminated Si(111) in contact with the aqueous solution but with no MV<sup>2+</sup> present (green dashed line).

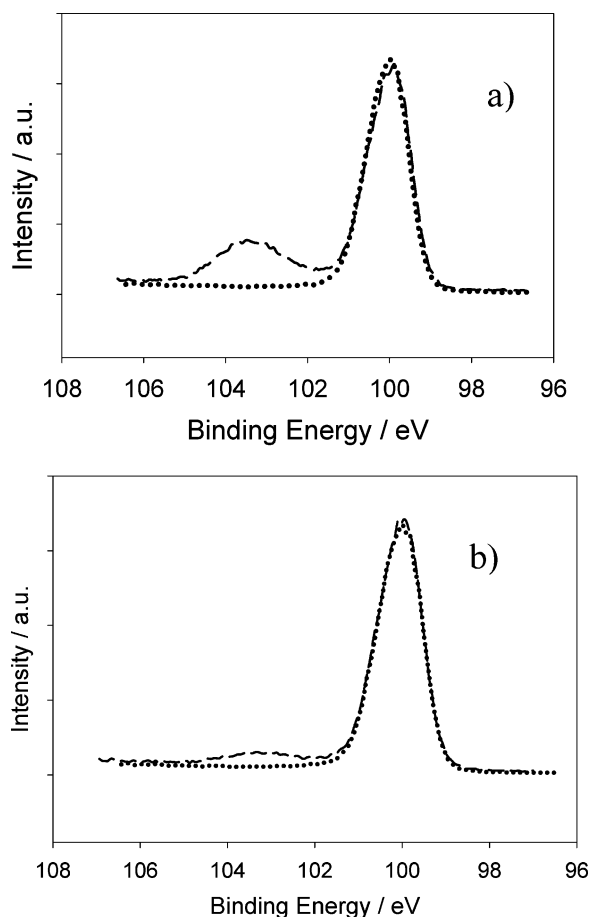
after. In fact, most H-terminated Si electrodes studied initially displayed  $J$ – $E$  curves with lower current densities at a given potential, being similar to the later scans of the  $J$ – $E$  curve shown in Figure 1.

Figure 2a displays XPS data (1487 eV Al K $\alpha$  excitation,  $\sim 0.5$  eV resolution)<sup>23,24</sup> in the Si 2p region of H–Si(111) samples before and after collection of the  $J$ – $E$  data. Si oxide was clearly observed after the  $J$ – $E$  measurements, even though extensive precautions were taken to prevent deliberate illumination of the electrode. The extent of oxidation was estimated by dividing the ratio of the SiO<sub>x</sub>:Si 2p peak areas by the normalization constant 0.21, as described previously.<sup>16</sup> Values of oxide coverage of greater than one equivalent monolayer, typically 1.2–1.8 equivalent monolayers, were observed after two  $J$ – $E$  scans at both 10 mM and 100 mM MV<sup>2+</sup> in the solution. This growth of an oxide peak is in agreement with the decay of the current during successive  $J$ – $E$  scans. Oxide was still formed even when the electrode was scanned only at relatively negative potentials ( $-0.5$  to  $-0.75$  V vs SCE). These results highlight the challenge of making reliable electrochemical measurements of H–Si(111) surfaces in contact with aqueous solutions. The pH dependence of Si electrodes reported previously<sup>9–11</sup> is then consistently ascribed to the presence of an oxide overlayer on the Si surface after it is initially used as an electrode in such aqueous solutions.

Figure 2b compares the high-resolution XPS data of the Si 2p region of CH<sub>3</sub>–Si(111) samples with those of freshly prepared H–Si(111) surfaces. 0.2–0.5 monolayer equivalents of silicon oxide were observed following 2 to 10  $J$ – $E$  scans at [MV<sup>2+</sup>] = 10 mM and [MV<sup>2+</sup>] = 100 mM. The introduction of the methyl functionality onto the silicon surface clearly inhibited oxidation of the Si, in accord with the stability of the  $J$ – $E$  curves for the CH<sub>3</sub>–Si(111) surfaces displayed in Figure 1. This behavior is in accord with the stability toward oxidation of alkyl-terminated Si(111) photoanodes under illumination.<sup>25,26</sup>

The inhibition of oxidation enabled the measurement of interfacial electron-transfer processes that were in accord with the ideal model of electron transfer at the semiconductor/liquid interface. The current density for an electron-transfer process from the conduction band of an n-type semiconductor to an acceptor species, A, in solution, is given by

$$J(E) = -qk_{ct}[A]n_s \quad (1)$$



**Figure 2.** High-resolution XPS data (using 1487 eV Al K $\alpha$  excitation) of the Si 2p region of: (a) a freshly etched H-Si(111) electrode (dotted line) and the electrode following  $J$ - $E$  measurements consisting of two scans at 10 mV s $^{-1}$  (dashed line); (b) a freshly etched H-Si(111) electrode (dotted line) and a methyl-terminated Si(111) electrode following  $J$ - $E$  measurements consisting of 2 scans at 10 mV s $^{-1}$  (dashed line).

where  $q$  is the charge of an electron ( $1.6022 \times 10^{-19}$  C),  $k_{\text{et}}$  is the electron-transfer rate constant ( $\text{cm}^4 \text{s}^{-1}$ ),  $[A]$  is the acceptor concentration ( $\text{cm}^{-3}$ ), and  $n_s$  is the electron concentration ( $\text{cm}^{-3}$ ) at the surface of the semiconductor.<sup>2</sup> The rate law of eq 1 can be demonstrated to apply by verification of the first-order dependence of  $J$  on  $[A]$  and  $n_s$ .<sup>27</sup>

According to eq 1, an increase in  $[A]$  by a factor of 10 should produce a potential shift,  $\Delta E$ , by  $(k_B T/q) \ln(10)$  (with  $k_B$  being Boltzmann's constant), i.e., by 59 mV at room temperature, to produce a given value of  $J$ . Figure 3 displays a semilogarithmic plot of  $J$  vs.  $E$  for a CH $_3$ -terminated Si(111) electrode in contact with solutions having  $[MV^{2+}] = 10$  mM and  $[MV^{2+}] = 100$  mM, respectively. The 10-fold increase in  $[A]$  resulted in a 50 mV shift of the  $J$ - $E$  curve, verifying the first-order dependence of  $J$  on  $[A]$ .

All of the junctions showed rectifying behavior in accord with the diode equation:

$$J = -J_0 (e^{(-qE)/\gamma k_B T} - 1) \quad (2)$$

where  $J_0$  is the exchange current density and  $\gamma$  is the diode quality factor. For CH $_3$ -terminated Si(111) surfaces, the diode quality factors were typically 1.1–1.3 at low concentrations of acceptor, in accord with the expectation of  $\gamma = 1$  for a process that is kinetically first order in the concentration of electrons at

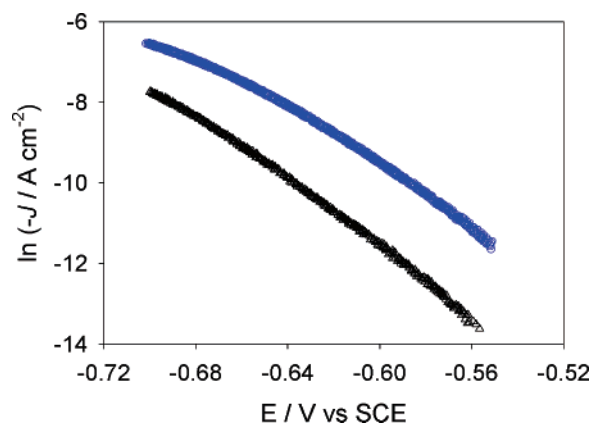


**Figure 3.** Semilogarithmic plots of  $J$  vs  $E$  for a methyl-terminated Si electrode at  $MV^{2+}$  concentrations of 10 mM (black triangles) and 100 mM (blue circles). As noted in the text, a 10-fold increase in  $[A]$  should result in a shift of the  $J$ - $E$  curve by approximately  $\Delta E = 59$  mV.

the surface of the semiconductor. In contrast, H-Si(111) electrodes either displayed, or quickly decayed to, a value of  $\gamma \approx 2$ .

Large  $MV^{2+}$  concentrations, while favoring direct electron transfer, typically produced higher diode quality factors on CH $_3$ -Si(111) surfaces, indicating the presence of nonideal recombination pathways at high acceptor concentrations. This behavior is attributed to the small growth of oxide that could not be fully suppressed at high  $MV^{2+}$  concentrations. In addition, measurements of CH $_3$ -Si(111) electrodes in contact with the stronger oxidant, Ru(NH $_3$ ) $_6^{3+/2+}$ , exhibited  $\gamma \approx 2$ . A correlation between the value of the diode quality factor and Si oxide growth was thus observed, underscoring the necessity of using carefully prepared CH $_3$ -terminated Si electrodes to probe the kinetics of interfacial electron transfer at n-type (111)-oriented Si electrodes in aqueous solution.

A Mott-Schottky (differential capacitance vs potential) analysis of the flat-band potential of CH $_3$ -Si(111) surfaces was not possible because the necessary applied potentials led to oxidizing, anodic currents, even in the dark at all  $MV^{2+}/MV^+$  concentrations explored. This drawback precluded determination of the interfacial electron-transfer rate constant; however, the measured current densities (Figure 3) are consistent with a low barrier height contact for n-type CH $_3$ -Si(111)/H $_2$ O- $MV^{2+}/+$  contacts.

Because the kinetics of interfacial electron transfer are strongly dependent on the interfacial energetics,<sup>8,28</sup> the kinetics are a good, although indirect, probe of energetic variations. Figure 4 displays the  $J$ - $E$  data obtained at  $[MV^{2+}] = 10$  mM for  $1.5 \leq \text{pH} \leq 11$ . If the band edges were to shift with pH, a corresponding change in the applied potential would be needed to produce a given value of the interfacial current density, as has been observed for n-ZnO electrodes in contact with outer-sphere redox couples.<sup>8</sup> The invariance of the  $J$ - $E$  curves relative to a fixed reference potential, despite the nearly 10 pH unit variation in the solution and in the formal potentials of the H $^+$ /H $_2$  and O $_2$ /H $_2$ O redox couples, is strong evidence that the band edges of CH $_3$ -Si(111) electrodes are fixed with respect to pH changes. This behavior is in contrast to the pH dependence of the band edges that is observed for metal oxides and for unmodified Si electrodes in aqueous solution. The data thus indicate that the energetics of the band-edge positions relative to a pH-dependent redox couple can be manipulated by pH changes at the CH $_3$ -Si(111)/H $_2$ O interface.

n-Type Si electrodes have previously been coated with metal films to achieve enhanced stability under illumination.<sup>29–31</sup>

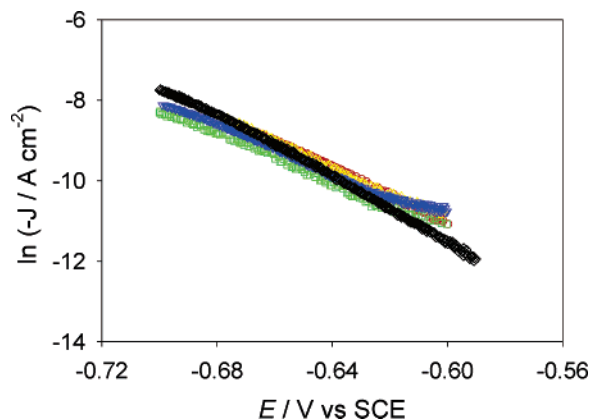


**Figure 4.** Semilogarithmic plots of  $J$  vs  $E$  for methyl-terminated Si electrodes in contact with 10 mM  $MV^{2+}$  at pH = 1.4 (blue upside down triangle), pH = 3.8 (green square), pH = 6.8 (yellow triangle), pH = 9.0 (red circle), and pH = 11.0 (black diamond).

Intimate contact of Si with a metal produces a floating junction in which the liquid does not control the energetics of the interface, and which suffers from majority-carrier-based thermionic emission type recombination at the regions having metal/Si contacts. In this work, control of the band-edge energies has instead been achieved by manipulation of the interfacial chemistry of the surface as well as the redox potential of the electrolyte. Functionalization of the Si to introduce Si–C bonds, along with further elaboration of the chemistry of such interfaces,<sup>23,24,32</sup> is therefore an interesting approach to control the properties of such semiconductor/liquid contacts.

#### IV. Conclusions

Methyl-terminated Si(111) electrodes have been demonstrated to effectively inhibit the oxidation of Si in contact with  $MV^{2+}$  dissolved in aqueous solutions. Such surface modification allowed for observation of current density vs applied potential behavior in accord with the ideal model of interfacial electron-transfer reactions at a semiconductor/liquid junction. The kinetics were observed to be independent of pH over approximately 10 pH units. Because the kinetics are dependent on the interfacial energetics, the invariance of the kinetics with respect to pH implies that the band-edge energetics of these modified Si surfaces are also independent of pH.

**Acknowledgment.** We acknowledge the NSF, grant CHE-0604894, for support of this work. XPS data were collected at the Molecular Materials Research Center of the Beckman Institute of the California Institute of Technology.

#### References and Notes

(1) Gerischer, H. In *Solar Energy Conversion. Solid-State Physics Aspects*; Seraphin, B. O., Ed.; Springer-Verlag: Berlin, 1979; Vol. 31, p 115.

- (2) Tan, M. X.; Laibinis, P. E.; Nguyen, S. T.; Kesselman, J. M.; Stanton, C. E.; Lewis, N. S. *Prog. Inorg. Chem.* **1994**, *41*, 21–144.
- (3) Bard, A. J.; Faulkner, L. R. *Electrochemical Methods, Fundamentals and Applications*; 2nd ed.; John Wiley & Sons: New York, 2001.
- (4) Bolts, J. M.; Wrighton, M. S. *J. Phys. Chem.* **1976**, *80*, 2641–2645.
- (5) Lohmann, F. *Ber. Bunsen-Ges. Phys. Chem.* **1966**, *70*, 428–434.
- (6) Morrison, S. R. *Electrochemistry at Semiconductor and Oxidized Metal Electrodes*; Plenum: New York, 1980.
- (7) Khaselev, O.; Turner, J. A. *Science* **1998**, *280*, 425–427.
- (8) Hamann, T.; Gstrein, F.; Brunenschwig, B. S.; Lewis, N. S. *Chem. Phys.* **2006**, *326*, 15–23.
- (9) Nakato, Y.; Ueda, T.; Egi, Y.; Tsubomura, H. *J. Electrochem. Soc.* **1987**, *134*, 353–358.
- (10) Madou, M. J.; Loo, B. H.; Frese, K. W.; Morrison, S. R. *Surf. Sci.* **1981**, *108*, 135–152.
- (11) Schlichthorl, G.; Peter, L. M. *J. Electrochem. Soc.* **1994**, *141*, L171–L173.
- (12) Bansal, A.; Li, X. L.; Lauermaun, I.; Lewis, N. S.; Yi, S. I.; Weinberg, W. H. *J. Am. Chem. Soc.* **1996**, *118*, 7225–7226.
- (13) Blackburn, G. F. In *Biosensors Fundamentals and Applications*; Turner, A. P. F., Karube, I., Wilson, G. S., Eds.; Oxford University Press: Oxford, 1987, pp 481–530.
- (14) Hafeman, D. G.; Parce, J. W.; McConnell, H. M. *Science* **1988**, *240*, 1182–1185.
- (15) Cui, Y.; Wei, Q. Q.; Park, H. K.; Lieber, C. M. *Science* **2001**, *293*, 1289–1292.
- (16) Webb, L. J.; Lewis, N. S. *J. Phys. Chem. B* **2003**, *107*, 5404–5412.
- (17) Webb, L. J.; Nemanick, E. J.; Biteen, J. S.; Knapp, D. W.; Michalak, D. J.; Traub, M. C.; Chan, A. S. Y.; Brunenschwig, B. S.; Lewis, N. S. *J. Phys. Chem. B* **2005**, *109*, 3930–3937.
- (18) Lide, D. R., Ed. *CRC Handbook of Chemistry and Physics*; 81st ed.; CRC Press: Boca Raton, 2001.
- (19) Dominey, R. N.; Lewis, N. S.; Bruce, J. A.; Bookbinder, D. C.; Wrighton, M. S. *J. Am. Chem. Soc.* **1982**, *104*, 467–482.
- (20) Bookbinder, D. C.; Bruce, J. A.; Dominey, R. N.; Lewis, N. S.; Wrighton, M. S. *Proc. Natl. Acad. Sci. U.S.A.* **1980**, *77*, 6280–6284.
- (21) Bocarsly, A. B.; Bookbinder, D. C.; Dominey, R. N.; Lewis, N. S.; Wrighton, M. S. *J. Am. Chem. Soc.* **1980**, *102*, 3683–3688.
- (22) Bookbinder, D. C.; Lewis, N. S.; Bradley, M. G.; Bocarsly, A. B.; Wrighton, M. S. *J. Am. Chem. Soc.* **1979**, *101*, 7721–7723.
- (23) Nemanick, E. J.; Hurley, P. T.; Brunenschwig, B. S.; Lewis, N. S. *J. Phys. Chem. B* **2006**, *110*, 14800–14808.
- (24) Nemanick, E. J.; Hurley, P. T.; Webb, L. J.; Knapp, D. W.; Michalak, D. J.; Brunenschwig, B. S.; Lewis, N. S. *J. Phys. Chem. B* **2006**, *110*, 14770–14778.
- (25) Bansal, A.; Lewis, N. S. *J. Phys. Chem. B* **1998**, *102*, 4058–4060.
- (26) Bansal, A.; Lewis, N. S. *J. Phys. Chem. B* **1998**, *102*, 1067–1070.
- (27) Fajardo, A. M.; Lewis, N. S. *J. Phys. Chem. B* **1997**, *101*, 11136–11151.
- (28) Hamann, T.; Gstrein, F.; Brunenschwig, B. S.; Lewis, N. S. *J. Am. Chem. Soc.* **2005**, *127*, 7815–7824.
- (29) Fan, F. R. F.; Keil, R. G.; Bard, A. J. *J. Am. Chem. Soc.* **1983**, *105*, 220–224.
- (30) Fan, F. R. F.; Hope, G. A.; Bard, A. J. *J. Electrochem. Soc.* **1982**, *129*, 1647–1649.
- (31) Fan, F. R. F.; Wheeler, B. L.; Bard, A. J.; Noufi, R. N. *J. Electrochem. Soc.* **1981**, *128*, 2042–2045.
- (32) Hurley, P. T.; Nemanick, E. J.; Brunenschwig, B. S.; Lewis, N. S. *J. Am. Chem. Soc.* **2006**, *128*, 9990–9991.